THE GENERATION OF Al_mFe IN DILUTE ALUMINIUM ALLOYS WITH DIFFERENT GRAIN REFINING ADDITIONS

M. W. Meredith[1], A. L. Greer[1] P. V. Evans[2] and R. G. Hamerton[2]

[1]University of Cambridge
Department of Materials Science and Metallurgy
Pembroke Street
Cambridge CB2 3QZ, UK

[2]Alcan International Limited
Banbury Laboratory
Southam Road
Banbury OX16 7SP, UK

Abstract

$Al_{13}Fe_4$, Al_6Fe and Al_mFe are common intermetallics in commercial AA1XXX series Al alloys . Grain-refining additions (based on either Al-Ti-B or Al-Ti-C) are usually added to such alloys during solidification processing to aid the grain structure development. They also influence the favoured intermetallic and, hence, can affect the materials' properties. This work simulates commercial casting practices in an attempt to determine the mechanisms by which one intermetallic phase is favoured over another by the introduction of grain-refining additions. Directional solidification experiments on Al-0.3wt.%Fe-0.15wt.%Si with and without grain refiner are conducted using Bridgman apparatus. The type, amount and effectiveness of the grain-refining additions are altered and the resulting intermetallic phase selection followed. The materials are characterised using optical microscopy, scanning electron microscopy and X-ray diffraction. Al_mFe is seen to form when Al-Ti-B grain-refiner is introduced but only when the refinement is successful; reducing the effectiveness of the refiner led to Al_6Fe forming under all conditions. Al-Ti-C refiners are seen to promote Al_mFe at lower solidification velocities than when Al-Ti-B was used even though the grain structure was not as refined. These trends can be explained within existing eutectic theory, by considering growth undercooling .

Light Metals 1999

Introduction

Grain-refiners are added to dilute aluminium alloys during the early stages of solidification processing to produce a predictable, equiaxed grain structure. The mechanisms by which this is achieved have been widely explored recently [1,2]. However, as well as aiding nucleation of ccp-Al, there is a less desirable effect of such additions; this is their influence on second-phase intermetallic particles during the latter stages of solidification. Figure 1 details some of the many binary and ternary intermetallic phases which may form in AA1XXXX series alloys [3,4,5]. The control of these in the final microstructure is fundamental in governing the properties of the material.

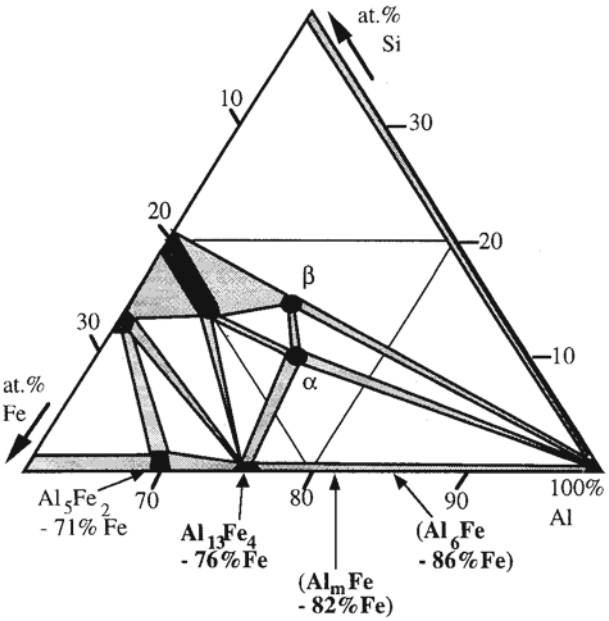

Figure 1: Isothermal section (500°C) through the Al-Fe-Si equilibrium phase diagram at the Al-rich corner. Metastable phases are shown in parentheses; phases of interest are shown in bold.

As these intermetallics cannot be removed once present (although they can be transformed to other intermetallics given sufficient time at temperature), it is crucial to control the various solidification parameters to produce the desired microstructure. A lack of control can result in the formation of more than one intermetallic [6,7], and in the material's properties being less predictable [8].

In an attempt to investigate how solidification conditions influence intermetallic selection, many researchers have employed controlled directional solidification techniques such as Bridgman solidification [9-14]. Generally, it is found that for a non-refined AA1XXX series alloy, the equilibrium phase $Al_{13}Fe_4$ gives way to Al_6Fe as the favoured binary intermetallic as the solidification conditions become more extreme. When grain-refiner is added Al_6Fe again supersedes $Al_{13}Fe_4$, but is itself replaced as conditions become more extreme by the other metastable binary intermetallic, Al_mFe. In commercial casting, there is a range of solidification velocities [15] and hence a range of intermetallic phases may form across an ingot. The transition from one intermetallic to another rarely occurs at a consistent depth from the ingot surface, leading to the "Fir-Tree Zone"[7] on etching of an ingot cross-section. Common practice during processing is to "scalp" the ingot (strip off the outer 10-20 mm of the ingot surface) to remove any inhomogeneities within the surface region such as a segregate layer or a shell zone of coarse cell structure. If the scalping plane intersects the fir-tree zone, the surface properties of the product in its final form will be inconsistent. Hence, control of the intermetallic selection at higher velocities in the presence of grain-refiner is crucial.

This work details recent investigations into the influence of different grain refining practices on intermetallic phase selection in dilute Al alloys. It is known that successful grain refinement of these alloys can result in the formation of the metastable phase Al_mFe, but it is unclear whether it is the presence of the refining particles or the resultant grain structure refinement which is responsible. The experimental work is split into four sections. Firstly, the influence of composition and grain-refining on eutectic characteristics (morphology and spacing) is investigated by deliberately producing the same intermetallic, Al_6Fe, under a number of different conditions; subsequent modelling of this eutectic system would suggest how the growth of this phase has been affected by the presence and morphology of the ccp-Al phase. Secondly, the level of Al-Ti-B addition is varied to produce a whole range of microstructures from fully columnar to fully refined; this should indicate whether the presence of chemically active grain-refining particles in a non-refined microstructure can generate Al_mFe or whether the morphology of the primary ccp-Al plays a part in the phase change. Thirdly, a level of Al-Ti-B refiner is added which is known to generate Al_mFe under certain solidification conditions, but then deliberately killed to reduce its effectiveness; analysis of the intermetallics in such a structure should indicate whether this level of addition can still generate Al_mFe in a non-refined structure. Finally, an Al-Ti-C grain refiner was used to ascertain whether the intermetallic phase selection was specific to a given type of grain-refiner.

Experimental Details

• Eutectic characteristics of Al_6Fe: a range of alloys, from fully eutectic (Al-3.0 wt.%Fe), through those with a large volume fraction of columnar primary phase (Al-0.5wt.%Fe, Al-0.5wt.%Fe-0.1wt.%Si), to a grain-refined example (Al-0.5wt.%Fe-0.1wt.%Si plus 10 parts per thousand (ppt) Al-Ti-B grain refiner) were prepared for directional solidification from 99.999% purity elemental components and then swaged down to the correct dimensions for Bridgman growth. The Bridgman furnace used was that at the Banbury Laboratory of Alcan International Ltd and has been described elsewhere [14]. Each alloy was grown at two different speeds (50 and 90 mm min^{-1}). The spacing of the eutectic microstructure was then assessed.

The bulk alloy for the rest of the experiments was Al-0.3wt.%Fe-0.15wt.%Si. The different grain-refining additions and solidification conditions were as follows:

• Varying grain-refiner level experiments: 3:1 Al-Ti-B grain-refiner was added to levels of 0, 1, 2, 3, 5, 8 and 10 parts per thousand (ppt). Each sample was then grown at 80 mm min^{-1} after having been held at 800°C for 5 minutes within the Bridgman furnace, conditions known to generate Al_mFe at the highest addition level.

• Killed grain-refiner experiments: 3:1 Al-Ti-B grain-refiner was added to a level of 10 ppt. The samples were then held at 900°C for 30 minutes in the Bridgman furnace to reduce the effectiveness of the refiner. They were subsequently grown at 40, 60 or 80 mm min^{-1}.

• Different grain-refiner investigations: 3:0.25 Al-Ti-C grain-refiner was added to a level of 20 ppt. Because this type of grain-refiner is more susceptible to temperature, the samples were held at a reduced temperature 720°C, for 5 minutes before growth at either 40, 60 or 80 mm min^{-1}.

Analysis of the samples in these three grain-refiner investigations was conducted in 2 stages. Firstly, the grain structure was checked to make sure that the required level of refinement in each experiment had been achieved. To this end, mounted, polished and anodised samples were examined by optical microscopy under plane-polarised light. If the appropriate grain structure had been generated, the intermetallic phases were then analysed. They were first extracted from the matrix using the SIBUT dissolution method [16]. In this process, small sections of the Bridgman-grown specimen were placed in a sealed autoclave of hot, anhydrous butanol. Over the course of several hours, the butanol dissolved the matrix but not the intermetallic phase; this was collected on a filter in the base of the autoclave and then dried once the reaction had finished. This extractate could then be analysed using X-ray diffraction. A Philips PW80 diffractometer was used to obtain XRD traces over a range 15-60° with CuK_α radiation.

Results

• Eutectic characteristics of Al_6Fe:

Figure 2 gives examples of the changing nature of the intermetallic phase as the composition is altered. Spacing measurements from such microstructures are given in Table 1. It is clear that each addition to the composition has resulted in the Al_6Fe eutectic spacing becoming wider. The morphology of the eutectic has also changed from rod-like, the traditional Al_6Fe morphology, to lamellar with the addition of Si and grain refiner.

alloy:	solidification velocity (mm/min): 50	90
Al-3.0wt.%Fe	0.40 µm	0.30 µm
Al-0.5wt.%Fe	0.59 µm	0.37 µm
Al-0.5wt.%Fe -0.1wt.%Si	0.94 µm	0.79 µm
Al-0.5wt.%Fe -0.1wt.%Si plus 10ppt 3:1 Al-Ti-B GR	1.30 µm	0.98 µm

Table 1: Al_6Fe eutectic spacing measurements as composition and solidification conditions change.

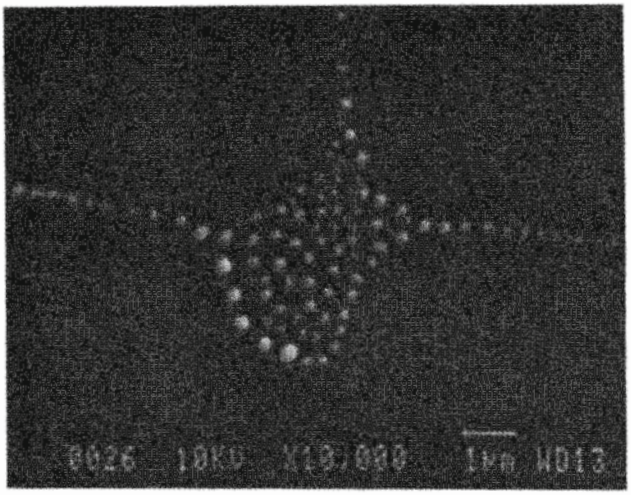

(a) non-grain-refined Al-0.5wt.%Fe

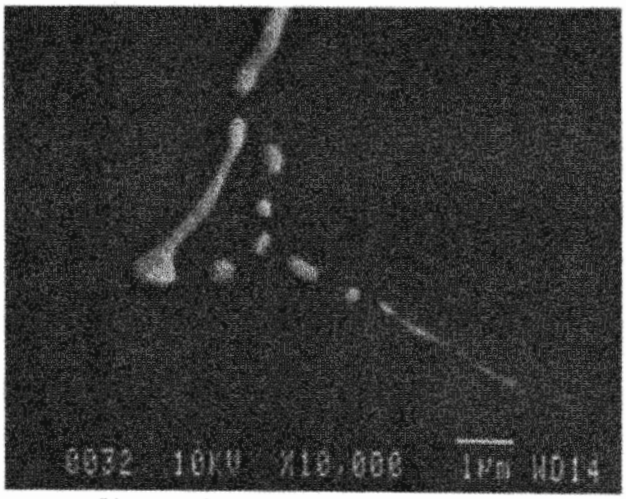

(b) non-grain-refined Al-0.5wt.%Fe-0.1wt%Si

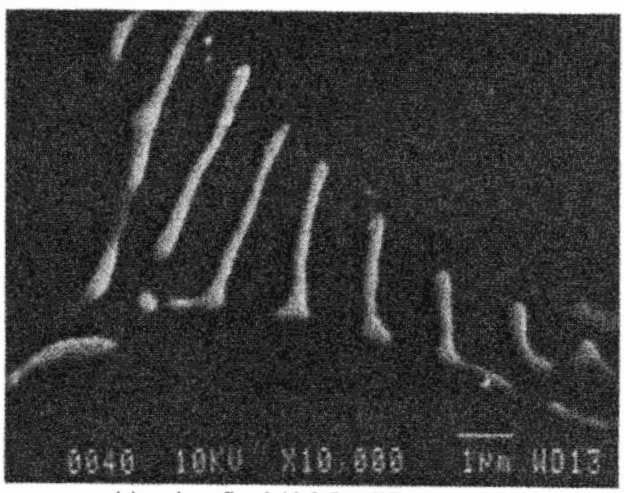

(c) grain-refined Al-0.5wt.%Fe-0.1wt%Si

Figure 2: Change in intermetallic morphology on the introduction of Si and grain refiner. All samples were grown at 50 mm min^{-1}.

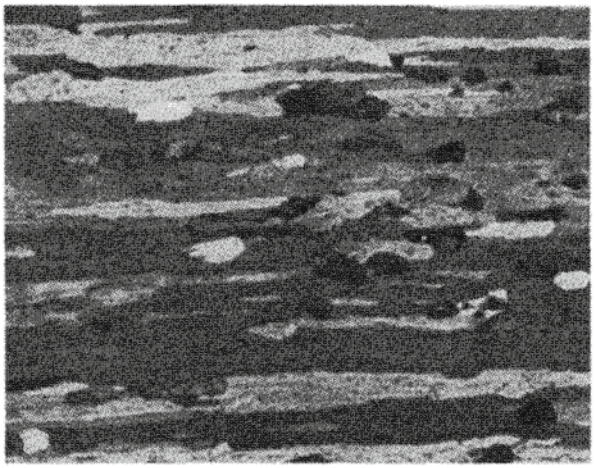

(a) 1 ppt

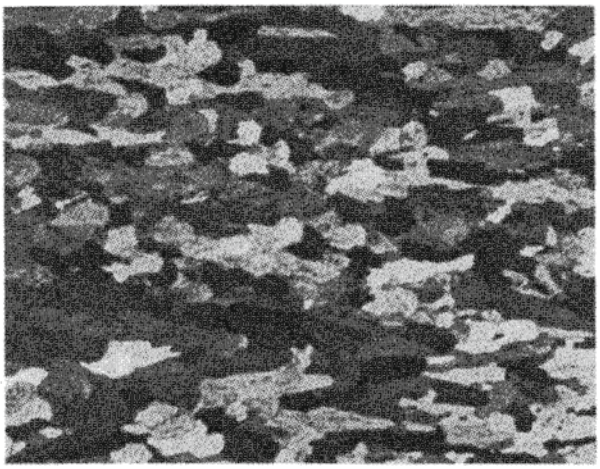

(b) 3 ppt

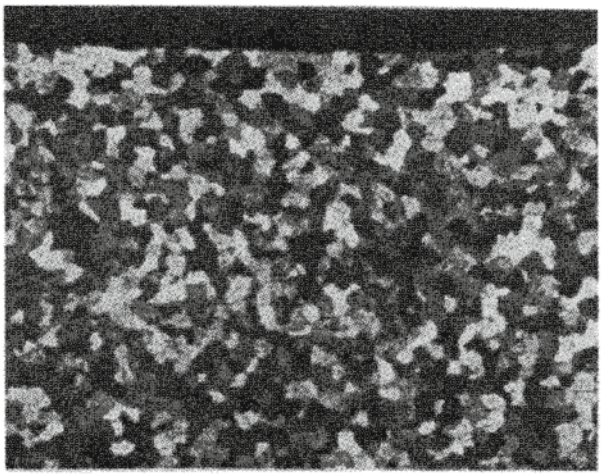

(c) 10 ppt — 20 µm

Figure 3: Grain structures obtained when varying levels (1, 3, and 10 ppt) of Al-Ti-B grain refiner are added. All the samples were grown at 80 mm min^{-1}.

• Varying grain-refiner level experiments:

Figure 3 gives examples of the grain structure generated when the level of grain-refiner addition is gradually changed. At a low level of refiner (1 ppt - fig.3a), isolated equiaxed grains appear within a matrix of larger columnar grains suggesting that, although nucleation of equiaxed grains is possible, their growth is not enough to consume the whole microstructure. The columnar grains soon disappear (fig.3b) but it is not until the grain-refiner level reaches ≥ 8 ppt that the grain structure appears completely refined (fig.3c).

Table 2 details how the phase selection changes as the refiner level is changed. At low levels (≤ 3 ppt), Al_6Fe is the dominant intermetallic with a gradual increase in the amount of α-AlFeSi which is present. At higher addition rates, the ternary phase then dominates but Al_mFe appears when the microstructure is completely refined (at ≥8 ppt). Al_6Fe is present throughout.

• Killed grain-refiner experiments:

Even after a substantial hold at an elevated temperature, the grain-refining ability of the Al-Ti-B inclusions is not completely killed (fig. 4). It has, however, been significantly reduced. The X-ray analysis confirms that this reduction has effected an intermetallic phase change (see Table 2). $Al_{13}Fe_4$ gives way to Al_6Fe and α–AlFeSi at the lower velocities (≤ 60 mm min^{-1}) but, unlike the previous example, Al_mFe does not appear after solidification at the highest velocity. At 80 mm min^{-1}, Al_6Fe is still the dominant intermetallic.

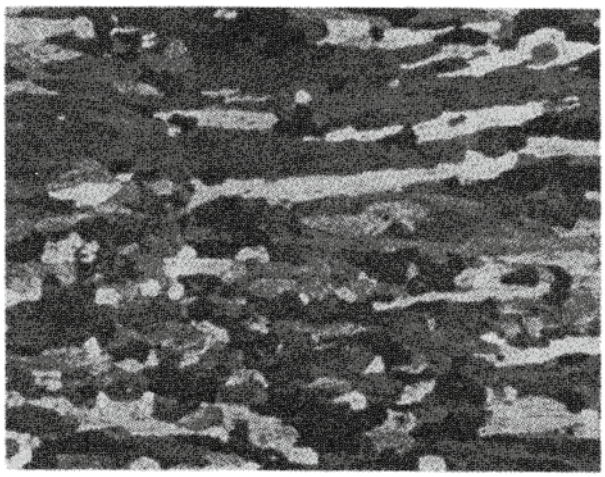

20 µm

Figure 4: Grain structure produced when the potency of the Al-Ti-B refiner is reduced. The material was grown at 60 mm min^{-1}.

• Different grain refiner experiments:

Even though the furnace conditions prior to solidification were less extreme and the Al-Ti-C grain refiner addition rate was high, the grain structure generated was not as refined as those produced with Al-Ti-B refiners (fig. 5). However, an intermetallic phase change was again noted as the solidification conditions changed. (see Table 2). As the velocity increased, $Al_{13}Fe_4$ was replaced by Al_mFe as the major intermetallic phase. Furthermore, this change was observed at a low solidification velocity (60 mm min^{-1}). α–

AlFeSi was always present as a minor phase. It is interesting to note that Al_6Fe was eliminated completely from all the microstructures.

	Solidification Velocity (mm/min)		
	40	60	80
varying grain-refiner levels: (ppt Al-Ti-B)			
0			6, α
1			6, α
2			6, α
3			6, α
5			α, 6
8			α , 6, m
10			α , 6, m
killed refiner expts: 10 ppt Al-Ti-B	3, 6, α	6, α	6, α
20 ppt Al-Ti-C	3, α	m, α	m, α

Table 2: Phase selection in grain-refiner experiments.

Discussion

Investigations into the intermetallic phase selection in dilute Al alloys have been ongoing for a number of years. The original analyses on commercially cast material were conflicting [7, 8, 17, 18] and it became apparent that close control of composition and solidification conditions was necessary for meaningful results to be obtained. This was much more easily done through laboratory simulations and recent such investigations [19-22] have led to intermetallic selection in these alloys being carefully mapped. The role played by successful grain-refinement of the alloys is still unclear.

The phases of interest in this study all form in the latter stages of solidification through eutectic reactions which consume the remaining solute-enriched liquid which occupies approximately 5-10% of the total volume. The faster solidification is driven, the further from equilibrium it occurs and, hence, the likelihood of metastable phases, such as Al_6Fe and Al_mFe, occurring increases. The model most often used for eutectic growth, usually in fully eutectic systems, is that developed by Jackson and Hunt [23]. They recognised the presence of three different components which built up the overall undercooling term, ΔT:

$$\Delta T = \Delta T_t + \Delta T_c + \Delta T_k \quad (1)$$

where ΔT_t, ΔT_c and ΔT_k are the contributions related to constitutional effects, curvature effects and kinetic effects respectively. The last of these is of minimal importance and can be ignored. Thus, equation (1) can be reduced to one of the type:

$$\Delta T = m_x\left[C_{x,e} - C_{x,i}\right] + \frac{a}{r} \quad (2)$$

m_x is the liquidus slope; $C_{x,e} - C_{x,i}$ is the difference between far-field and interface liquid compositons; a is a constant related to the Gibbs-Thomson coefficient; and r is the radius of curvature of the interface. By considering the differing influences of constitution and curvature and assuming that growth of the eutectic phase occurs at the extremum (for example, at the minimum undercooling for any given solidification velocity), Jackson and Hunt derived a set of three mutually compatible equations describing growth of a given eutectic in terms of undercooling, ΔT, solidification velocity, v, and eutectic spacing, λ:

$$\lambda^2 v = a/Q \quad (3a)$$

$$\Delta T / \sqrt{v} = 2m\sqrt{a.Q} \quad (3b)$$

$$\Delta T.\lambda = 2m.a \quad (3c)$$

Q is a constant term related to the diffusion of a given elemental species in the liquid; m is an average of the ccp-Al and intermetallic liquidi. Even though the model was primarily developed for planar growth in a fully eutectic binary system, it can be simply be modified to indicate how a third component, or other inclusions such as grain-refiner additions, might influence the eutectic growth in the system [24]. For example, equation (3b) can be extended to incorporate the constitutional effects of a third component:

$$\Delta T = 2m\sqrt{a.Q}.\sqrt{v} + m_y\left[C_{y,e} - C_{y,i}\right] \quad (4)$$

Assuming the eutectic growth to be planar, and given knowledge about the constants a and Q, equation (4) can be used to predict how the growth temperature of a number of eutectic systems would vary with velocity. Such variations can be seen in fig.6(a) as calculated for the different eutectics in the Al-Fe system.

When considering competition of different eutectics within the same system, it is assumed that, at any given velocity, the eutectic which can grow at the smallest undercooling will predominate. Figure 6(a) indicates that, at the lower velocities, the equilibrium phase $Al_{13}Fe_4$ is favoured, but as the velocity increases Al_6Fe will form due to a relatively low diffusion-related constant. Importantly, though, it must be noted that if growth at the extremum is assumed, Al_mFe will not form under normal solidification conditions. It has recently been reported that it is possible to generate this phase in an Al-Fe binary alloy when production is via high-speed twin-roll casting [25]. However, solidification rates in this process (cooling rates of 10^4 °C s^{-1}) far exceed those experienced under normal solidificaiton conditions.

Experimental observations led Magnin and Trivedi [26] to conclude that growth of some eutectic systems was not occurring at the extremum but at some distance away from it as described by:

$$\lambda_{op} = \phi.\lambda \quad (5)$$

where ϕ is a measure of how removed from the extremum the eutectic is growing. If this is incorporated into equation (4), it becomes:

$$\Delta T = \left(\phi + \frac{1}{\phi}\right) 2m\sqrt{a.Q}.\sqrt{v} + m_y\left[C_{y,e} - C_{y,i}\right] \quad (6)$$

In this way, assuming that Al_6Fe grows at some distance away from the extremum, fig.6(b) can be generated which predicts the growth of Al_mFe at solidification velocities within the boundaries of conditions seen in commercial casting practices.

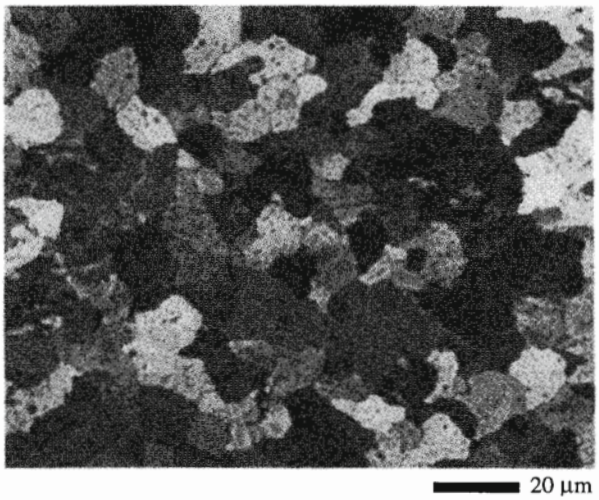

Figure 5: Grain structure obtained when 20 ppt Al-Ti-C grain-refiner is used. The sample was grown at 60 mm min^{-1}.

There is a great deal of experimental evidence [9, 21, 22] that the introduction of third components, such as Si, and grain-refiners alters the characteristics of the eutectic phases (for example, ΔT and λ). In general terms, such additions have been seen to restrict the formation of Al_6Fe but it is unclear why. Silicon in the liquid just ahead of the eutectic interface will increase the ΔT_t term and the magnitude of this effect will be influenced by back diffusion of the Si into the solid already formed [27] and the ability of each intermetallic to absorb Si. (Si will also be absorbed by the ccp-Al but this will be the same for each intermetallic.) More Si absorbed by the eutectic results in a lower ΔT_t term. Compositional analysis of the three binary intermetallics [28] reveals that Al_6Fe absorbs significantly less Si than $Al_{13}Fe_4$ or Al_mFe. Hence, it is likely that, when Al_6Fe forms, the additional constitutional undercooling terms caused by Si will be greater than if either $Al_{13}Fe_4$ or Al_mFe were forming; therefore, the growth front will become more depressed. Such a depression would enable Al_mFe to form at lower solidificaiton velocities.

The addition of Si has also been seen to influence the eutectic spacing. Figure 2 details the Al_6Fe intermetallic morphology in a range of Al-Fe(-Si) alloys. It is immediately apparent that the inclusion of Si has radically altered the nature of the intermetallic and the eutectic spacing has increased markedly. If the parameters within a and Q are unaltered by the presence of Si, the extension to the Jackson and Hunt eutectic theory given by equation 6 can be used to predict how far from the extremum conditions the eutectic is growing.

The role which grain-refining additions play in phase selection is less obvious as the introduction of such inclusions causes a change to two or three features concurrently (composition, grain structure, primary and eutectic growth front undercooling). The investigations described here go some way to separating out each effect. Al_mFe was seen to form in an alloy successfully refined by 10 ppt Al-Ti-B grain refiner but not to form when the same level of refiner was less effective (see figs.3 and 4 and table 2). The only difference between the two samples was the morphology of the ccp-Al so this must have played a part in the phase selection. The increase in eutectic spacing (as detailed in fig.2) suggests that refinement has led to growth of the eutectic away from the extremum. This could again result in the Al_6Fe growth front becoming depressed so that the formation of Al_mFe is possible. The experiments do indicate that any change in the constitutional undercooling term caused by the addition of grain-refiner is not enough, in itself, to promote an intermetallic phase change under these solidification conditions. When the microstructure is refined with Al-Ti-C additions, the Al_mFe appears at a lower velocity (60 mm min^{-1} as opposed to 80 mm min^{-1} for the Al-Ti-B additions) even though the refinement is not as effective. It is interesting to note that the excess level of Ti in the Al-Ti-C refiners is much higher than that in the Al-Ti-B refiners (2wt% and 0.8wt.% respectively of the refiner rod addition).

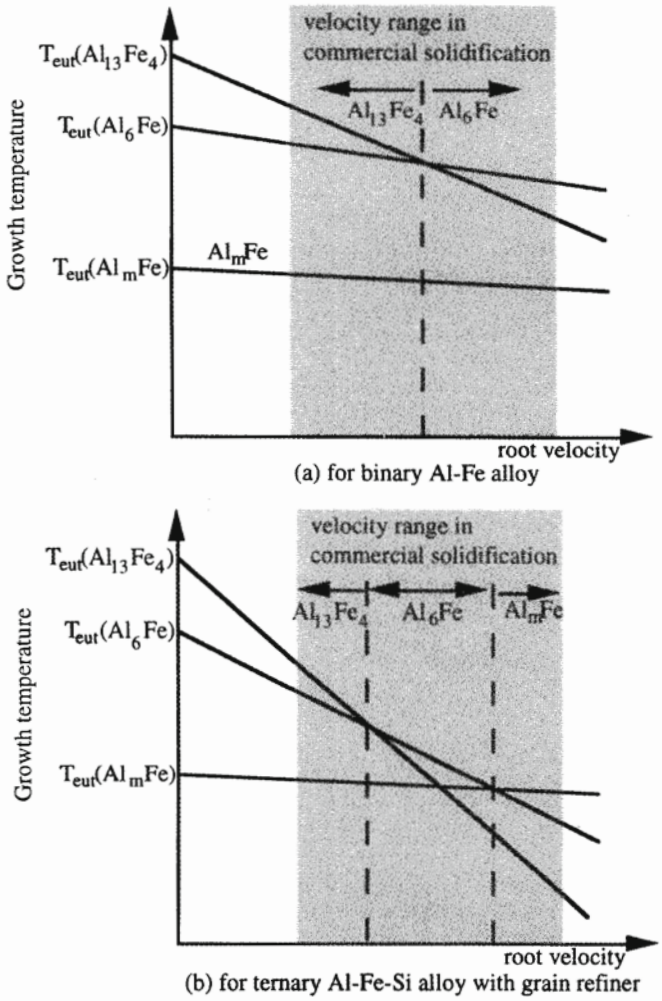

Figure 6: Schematic of how growth temperature and phase selection can change with solidification velocity and composition for Al-Fe(-Si) alloys.

Conclusions

In conditions closely resembling those experienced during commercial solidification practices, it is possible to generate Al_mFe as the predominant intermetallic in 1XXX Al-Fe-Si alloys. When the ternary Al-0.3wt.5Fe-0.15wt.%Si alloy is successfully refined, growth at a high speed results in the formation of this phase rather than Al_6Fe. The speed at which the phase first appears is dependent on which type of grain-refiner is used (80 or 60 mm min^{-1} for Al-Ti-B or Al-Ti-C grain refiners respectively). The reasons for this are unclear but constitutional undercooling considerations and growth of Al_6Fe away from the extremum conditons predicted for eutectic growth may play a part.

References

1. P. Schumacher and A. L. Greer, "Heterogeneously Nucleated α–Al in Amorphous Aluminium Alloys," Mater. Sci. Eng. A, A178 (1994) 309.

2. P. Schumacher and A. L. Greer, "Enhanced Heterogeneously Nucleated α–Al in Amorphous Aluminium Alloys," Mater. Sci. Eng. A, A181/A182 (1994) 1335.

3. G. Petzow and G. Effenberg, eds., Ternary Phase Diagrams, vol. 5 (New York, NY: VCH Publishers, 1992), 394.

4. E. H. Hollingsworth, G. R. Frank Jr., E. R. Willett, "Identification of a new Al-Fe Constituent, Al_6Fe," Trans. AIME, 224 (1962) 188.

5. P. Skjerpe, "Structure of Al_mFe," Acta Cryst., B44 (1988) 480.

6. D. Altenpohl, "Microstructural Examination of Cast Al," Z. Metallkde, 46 (1955) 535.

7. H. Westengen, "Formation of Intermetallic Compounds during DC-Casting of Commercial Al-Fe-Si alloys," Z. Metallkde, 73 (1986) 361.

8. H. Kosuge, "Intermetallics in the Al-Fe System," Keikenzoku, 30 (1990) 1.

9. P. V. Evans, J. Worth, A. Bosland and S.C. Flood, "Intermetallic Phase Selection in AA1XXXX Aluminium Alloys," Proceedings of the 4th Decennial International Conference on Solidification Processing, eds. J. Beech, H. Jones, Sheffield, University of Sheffield, 1997, 531.

10. D. Liang and H. Jones, "Morphologies of Primary Al_3Fe in Bridgman Solidification and TIG Weld Traversing of Hypereutectic Al-Fe Alloys," Mater. Sci. Eng A., A173 (1993) 109.

11. I. R. Hughes and H. Jones, "Coupled Eutectic Growth in Al-Fe Alloys," J. Mater. Sci., 11 (1976) 1781.

12. I. C. Stone and H. Jones, "Effect of Cooling Rate and Front Velocity on Solidification Microstructure Selection in Al-3.5%Fe-0 to 8.5%Si Alloys," Mater. Sci. Eng. A, A226-228 (1997) 33.

13. D. Liang, P. Korgul and H. Jones, "Composition and Solidification Microstructure Selection in the Interdendritic Matrix between Primary Al_3Fe Dendrites in Hypereutectic Al-Fe Alloys," Acta Mater., 44 (1996) 2999.

14. M. W. Meredith, A. L. Greer and P. V. Evans, "The Influence of Grain Refiner on Intermetallic Selection in Dilute Al-Fe alloys," Proceedings of the 4th Decennial International Conference on Solidification Processing, eds. J. Beech, H. Jones, Sheffield, University of Sheffield, 1997, 541.

15. I. Minkoff, Solidification and Cast Structure, (Chichester, UK: J. Wiley and Sons, 1983): Chapter 13.

16. C. J. Simensen, P. Fartum and A. Anderson, "The SIBUT Process," Frezenius Z. Anal. Chem., 319 (1984) 286.

17. S. Asami, T. Takana and A. Hideno, "Fir-tree structure in DC-cast ingot of Al-Mg-Fe-Si alloy," Keikenzoku, 28, 1978, 321.

18. S. Brusthaug, D. Porter and O. Vorren, "The effect of processing parameters on the fir tree structure in DC-cast rolling ingots," 8th International Light Metal Conference, Alverley, 1987, 472.

19. S. J. Maggs, "The Effect of Solidification Conditions on Nucleation of Al-Fe Intermetallics," (Ph.D Thesis, Leeds University, 1995), Chapter 4.

20. I. Todd and H. Jones, "The effect of cumulative alloying additions on intermetallic phase selection in alloys based on Al-0.5%Fe," Materials Science Forum, 217-22, 1996, 201.

21. M. W. Meredith, A. L. Greer and P. V. Evans, "The effect of grain-refining additions on intermetallic selection in dilute aluminium alloys," Light Metals 1998 (ed. B. Welch), The Minerals, Metals and Materials Society, 1998, 977.

22. R. W. Thomas, H. Cama, P. V. Evans and J. D. Hunt, "A Study of the Phases Found in Al Rich Al-Fe Alloys," Proceedings of the 4th Decennial International Conference on Solidification Processing, eds. J. Beech, H. Jones, Sheffield, University of Sheffield, 1997, 559.

23 K. A. Jackson and J. D. Hunt, "Lamellar and Rod Eutectic Growth," Metall. Trans., 226 (1966) 1129.

24. D. G. McCartney, J. D. Hunt and R. M. Jordan, "The structures expected in a simple ternary eutectic system: Part 1. Theory", Metall.. Trans. A, 11A, 1980, 1243.

25. R. W. Thomas, Ph.D thesis, Oxford University, 1998.

26. P. Magnin and R. Trivedi, "Eutectic growth: a modification of the Jackson and Hunt theory," Acta Metall. Mater., 39, 1991, 453.

27. T. W. Clyne and W. Kurz, "Solute redistribution during solidification with rapid solid state diffusion," Metall. Trans., 12A, 1981, 965.

28. Y. Langsrud, "Silicon in commercial aluminium alloys - what becomes of it during DC-casting," Key Eng. Mater., 44 & 45, (1990), 95.